INTERNATIONAL JOURNAL OF AUTOMOTIVE AND MECHANICAL ENGINEERING (IJAME)
ISSN: 2229-8649 e-ISSN: 2180-1606
VOL. 17, ISSUE 2, 7956 – 7966
DOI: https://doi.org/10.15282/ijame.17.2.2020.14.0595

ORIGINAL ARTICLE

Fatigue Life Analysis of Vehicle Systems under Non-Gaussian Excitation

Zhe Yang[1], Dapeng Zhu[2*], Quanfu Gao[1], Linqiang Gong[1], and Degong Xu[1]

[1]School of Mechanical Engineering, Lanzhou Jiaotong University, 730070, Lanzhou, China
[2]School of Traffic and Transportation, Lanzhou Jiaotong University,730070, Lanzhou, China

ABSTRACT – Fatigue life analysis is an important work in manufacturing of vehicle systems. The traditional method is to assume that stochastic loads are Gaussian type, then fatigue life is calculated by rain-flow counting, S-N curve and Miner linear damage rule. However, it is difficult to acquire accurate results by this means. In this paper, a numerical methodology is used to simulate non-Gaussian loads considering effects of skewness and kurtosis, as well as to estimate fatigue life under non-Gaussian stresses. Firstly, non-Gaussian inputs are represented by polynomial chaos expansion (PCE) and Karhunen-Loeve (KL) expansion when they are characterised using first four moments, i.e. mean, variance, skewness, kurtosis and a given correlation structure. During this process, we propose spectral decomposition to eliminate the influence of potential imaginary numbers, principal component analysis is also proposed to simplify calculating procedure in KL. Besides, original Monte Carlo sampling is replaced by quasi Monte-Carlo (QMC), which could greatly reduce the workload of numerical simulations. In order to get first four moments and correlation structure of outputs, differential equations of motion are numerically integrated by Runge-Kutta method. Meanwhile, response trajectories are represented based on PCE-KL-QMC approach. Eventually, the rain-flow counting is applied into these trajectories to obtain fatigue life variables, and a convenient formula about the saddlepoint approximations (SPA) represented by first four moments is proposed to provide fatigue life PDF. According to the above way, accurate and effective fatigue life estimation results can be presented.

ARTICLE HISTORY
Revised: 16th May 2020
Accepted: 23rd June 2020

KEYWORDS
Fatigue life estimation; Polynomial chaos expansion; Karhunen-Loeve expansion; Quasi Monte Carlo; Saddlepoint approximations

INTRODUCTION

The fatigue failure of vehicle components has long been considered as one of the main factors to cause accidents. Failure is a cumulative event that materials gradually produce brittle cracks and eventually break due to fluctuating stresses [1, 2]. In fact, fatigue failure of mechanical parts will not cause any obvious deformation, so fatigue life prediction is a significant job in the maintenance and operation of automotive.

In the past few years, many scholars have studied a series of problems in the prediction of vehicle fatigue life, mainly including simulation of random excitation, response analysis of vehicle components and fatigue life calculation methods. A moving car usually experiences non-Gaussian excitation in a real environment which is quite different from Gaussian that, so traditional Gaussian random signals could not represent these non-Gaussian processes. There are two different ways to simulate non-Gaussian excitation in literature [3, 4, 5, 6], one is on the foundation of first four moments and power spectral density, the other is based on probability density function and PSD. Response analysis is relatively simple; an overview is provided in [4, 7, 20].

There are lots of useful ways to predict fatigue damage in time and frequency domain in recent years. Frequency domain approaches [8, 9] can be generally used to predict fatigue damage based on PSD statistics, and the key is to construct a stress amplitude probability function model that meets requirements. The time-domain analysis evaluates fatigue life by describing the statistical law of stress change with time [9, 10], such as rain flow counting. This theory aims to convert an irregular, random load-time history into a series of cyclic processes, and it is convenient for computer programming. Dietz et al. proposed a way, combining frequency and time domain theory, to estimate the fatigue life of vehicle bogie. At the same time, this way was applied to work together with the computer-aided design, the finite element method and the multibody system program [11]. On the basis of measured pavement data of proving ground, Men et al. simulated road excitation under ADAMS environment, as well as calculated fatigue life according to the dynamic loads working on a vehicle air suspension [12]. In Ferreira et al.'s work, authors gave a comparative result about several automotive components fatigue life problems by time and frequency domain methods, where these problems involved not only static and dynamic behaviour but also single input and multiple correlated inputs [13].

From the literature [14], it has been concluded that damage accumulation is sensitive to non-Gaussian excitation. In view of this, we should hunt a new way to simulate non-Gaussian pavement excitation in line with the real environment. Subsequently, the accurate fatigue life of vehicle components could be obtained based on these simulated incentives. This paper aims to analyse the fatigue life of nonlinear vibratory systems under non-Gaussian loads. In the first place, non-Gaussian inputs are generally represented by polynomial chaos expansion and Karhunen-Loeve expansion, then

*CORRESPONDING AUTHOR | Dapeng Zhu | ✉ 2812014684@qq.com

parameters in these stochastic process expressions are acquired on the grounds of given first four moments and correlation structure. Numerical solutions of vehicle system differential equations are easily calculated on the foundation of fourth-order Runge-Kutta approach. From this, we can deduce the first four moments of outputs and even simulate response trajectories based on PCE-KL-QMC. Subsequently, each trajectory is rainflow cycle counted for the purpose of obtaining fatigue life random variables. In the end, saddlepoint approximations provide the life PDF.

ANALYSIS APPROACH OVERVIEW

Simulation of non-Gaussian Excitation

Vibration systems are often affected by non-Gaussian excitation. Generally speaking, a non-Gaussian process $F(t)$ has the same PSD, mean μ_F and variance σ_F^2 with a Gaussian process. Still, its other parameters, namely skewness and kurtosis, are not equal to 0 and 3 that belong to values of a Gaussian distribution. So the definitions of skewness S_F and kurtosis K_F in literature [3] are needed to character non-Gaussian properties of $F(t)$. Figure 1 shows the differences between non-Gaussian and Gaussian stochastic process.

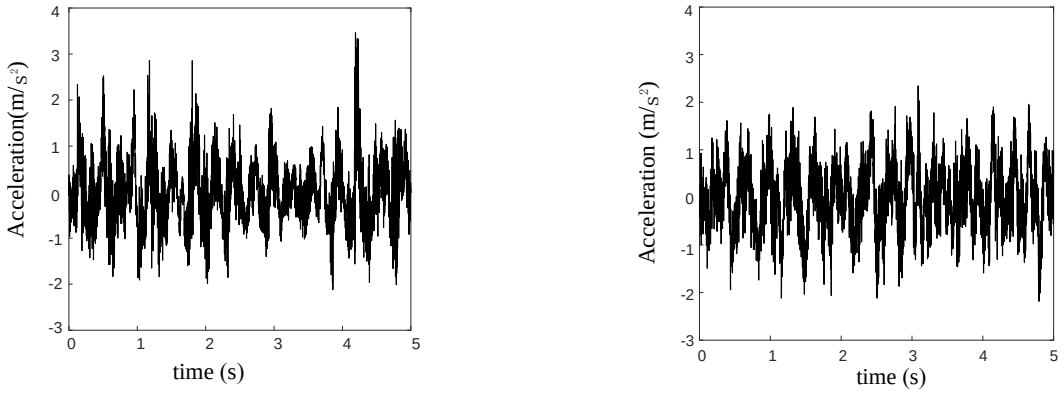

(a) non-Gaussian process (b) Gaussian process

Figure 1. Comparison between non-Gaussian and Gaussian process.

Autocorrelation function ρ_{FF} is the inverse Fourier transform of the targeted PSD. Using a time discretization $dt=\Delta t$ sec for the $0\leq t\leq T$ time of interest and $N=T/\Delta t+1$ is the number of sampling points. Afterwards, covariance matrix $C_{FF}(t_i,t_j)$, $i, j=1,\cdots,N$ is formed, where $C_{FF}(t_i,t_j)=\rho_{FF}(\tau)$ and $\tau=|t_i-t_j|=\Delta t|i-j|$. Then $\boldsymbol{\Sigma}_{\xi\xi}=[\boldsymbol{\Sigma}_{\xi\xi}(t_i,t_j)]$, the covariance of a standard normal process $\xi(t)$, is used to perform a spectral decomposition [15]:

$$\boldsymbol{\Sigma}_{\xi\xi}=Q\boldsymbol{\Sigma}Q^{\mathrm{T}} \tag{1}$$

where $\boldsymbol{\Sigma}=\mathrm{diag}(\lambda_1,\lambda_2,\cdots,\lambda_N)$ and $\lambda_1,\lambda_2,\cdots,\lambda_N$ are singular values of $\boldsymbol{\Sigma}_{\xi\xi}$, $Q=[Q_1, Q_2, \cdots, Q_N]$ and Q_i is singular vector, $i=1,2,\cdots,N$. In this way, $\xi(t)$ can be represented by Karhunen-Loeve expansion [4] based on independent standard normal variables u_i:

$$\xi(t)=\sum_{i=1}^{N}\sqrt{\lambda_i}\cdot Q_i(t)\cdot u_i \tag{2}$$

Principal component analysis plays an important role in determining the number of singular values, vectors and independent standard normal variables required in Eq.(2), then this problem is transformed to calculate the value of r in the following formula:

$$\left(\sum_{i=1}^{r}\lambda_i\cdot {Q_i}^2(t)\right)\Big/\left(\sum_{i=1}^{N}\lambda_i\cdot {Q_i}^2(t)\right)\geq p \tag{3}$$

where $0<p\leq 1$, a non-Gaussian variable F is usually expressed by the standard normal random variable ξ [16] :

$$F=\sum b_k H_k(\xi)=b_0+b_1\xi+b_2(\xi^2-1)+b_3(\xi^3-3\xi)+\cdots \tag{4}$$

where $b_k(k=0,1,2,3\cdots)$ are coefficients of polynomial chaos expansion. One-dimensional Hermite orthogonal polynomial $H_k(\xi)$ is defined as [5]:

$$H_k(\xi)=(-1)^k e^{\frac{\xi^2}{2}}\frac{d^k}{d\xi^k}e^{-\frac{\xi^2}{2}} \tag{5}$$

Equation (4) can be extended in time as:

$$F(t) = \sum b_k(t) H_k(\xi(t)) = b_0(t) + b_1(t)\xi(t) + b_2(t)(\xi(t)^2 - 1) + b_3(t)(\xi(t)^3 - 3\xi(t)) + \cdots \quad (6)$$

these coefficients b_k (k=0,1,2,3...) are constants for a stationary non-Gaussian process $F(t)$. Using the orthogonal properties of Hermite polynomial, the covariance $C_{FF}(t_i,t_j)$ with respect to t_i and t_j is equal to:

$$C_{FF}(t_i, t_j) = \sum_k b_k(t_i) b_k(t_j) \cdot (k!) \cdot (E[\xi(t_i)\xi(t_j)])^k \quad (7)$$

where $E[\zeta(t_i)\zeta(t_j)]=\boldsymbol{\Sigma}_{\xi\xi}(t_i,t_j)$, i,j=1,2,⋯,N. From this, $\boldsymbol{\Sigma}_{\xi\xi}$ in Eq.(1) is obtained and unknown coefficients b_1,b_2,b_3,b_4 are calculated according to the following equations:

$$\mu_F = E(F) = b_0 = g_1(b_0, b_1, b_2, b_3) \quad (8\text{-}1)$$

$$E[(F - \mu_F)^2] = {b_1}^2 + 2{b_2}^2 + 6{b_3}^2 = g_2(b_0, b_1, b_2, b_3) \quad (8\text{-}2)$$

$$E[(F - \mu_F)^3] = 6{b_1}^2 b_2 + 8{b_2}^3 + 36 b_1 b_2 b_3 + 108 b_2 {b_3}^2 = g_3(b_0, b_1, b_2, b_3) \quad (8\text{-}3)$$

$$E[(F - \mu_F)^4] = 3{b_1}^4 + 60{b_2}^4 + 3348\,{b_3}^4 + 60\,{b_1}^2{b_2}^2 + 252\,{b_1}^2{b_3}^2 + 576\,b_1{b_2}^2 b_3 + 1296\,b_1{b_3}^3 + 2232\,{b_2}^2{b_3}^2 = g_4(b_0, b_1, b_2, b_3) \quad (8\text{-}4)$$

Given the first four statistics parameters μ_F, σ_F^2, S_F and K_F, functions $gg_u(b_0,b_1,b_2,b_3)$, u = 1,2,3,4 are defined as:

$$\mu_F = E(F) = b_0 = g_1(b_0, b_1, b_2, b_3) \quad (9\text{-}1)$$

$$gg_2(b_0, b_1, b_2, b_3) = g_2(b_0, b_1, b_2, b_3) - \sigma_F^2 \quad (9\text{-}2)$$

$$gg_3(b_0, b_1, b_2, b_3) = g_3(b_0, b_1, b_2, b_3) - S_F\sigma_F^3 \quad (9\text{-}3)$$

$$gg_4(b_0, b_1, b_2, b_3) = g_4(b_0, b_1, b_2, b_3) - K_F\sigma_F^4 \quad (9\text{-}4)$$

The optimisation model f is then constructed:

$$f = \min_{b_0,b_1,b_2,b_3} \sum_{u=1}^{4} {gg_u}^2(b_0, b_1, b_2, b_3) \quad (10)$$

These coefficients b_0,b_1,b_2,b_3 are calculated by global optimisation methods, such as simulated annealing [17], which reduce the risk of getting a local optimal solution.

Response Analysis of Vibratory Systems

Monte Carlo (MC) approach, based on the idea of using sampling, aims to deal with mathematical problems that cannot be solved by analytical processes [18]. More precisely, this idea is to create samples that are used to derive approximations about a quantity of interest and its probability distribution. MC uses random sampling, which usually causes local aggregation of samples. In view of this, the quasi Monte Carlo method using low-discrepancy sampling is selected to improve the efficiency in multivariate integration evaluations. The specific steps are shown in Figure 2.

According to the QMC method [19], we should reasonably sample in the r-dimensional space $[0, 1]^r$. For that, a Latin Hypercube design is adopted, which can achieve the purpose of stratified sampling in computer experiments. In other words, it creates r sets or sequences of vectors. Therefore stochastic process $\xi(t)$ can be approximated by r standard normal variables. We construct a matrix $A=\{A_i=(A_{i,1},A_{i,2},\cdots A_{i,r}),\ i=1,2,\cdots n\}$ where elements in the row vector A_i obey uniform distribution from 0 to 1, as well as n is at least three to five times larger than r. Secondly, elements in A_i are substituted into the inverse standard normal cumulative distribution function $\Phi^{-1}(\cdot)$, then a new vector $\{u=(u_1,u_2,\cdots,u_r)\}$ is formed. The variables $u_j=\Phi^{-1}(A_{i,j})$, j=1,2,⋯r are used in Eq.(2) to obtain a process of $\xi(t)$ which in turn is used in Eq. (6) to get a non-Gaussian excitation. Following the above steps, row vectors of A are used for acquiring all non-Gaussian inputs $F_i(t)$, i=1,2,⋯n. Subsequently, establishing motion differential equations, and output trajectories $X_i(t)$ are obtained due to the fourth-order Runge-Kutta algorithm where time interval [0, T] is divided by a step Δt so that $t_j=(j\text{-}1)\Delta t$, j=1,2,…,N.

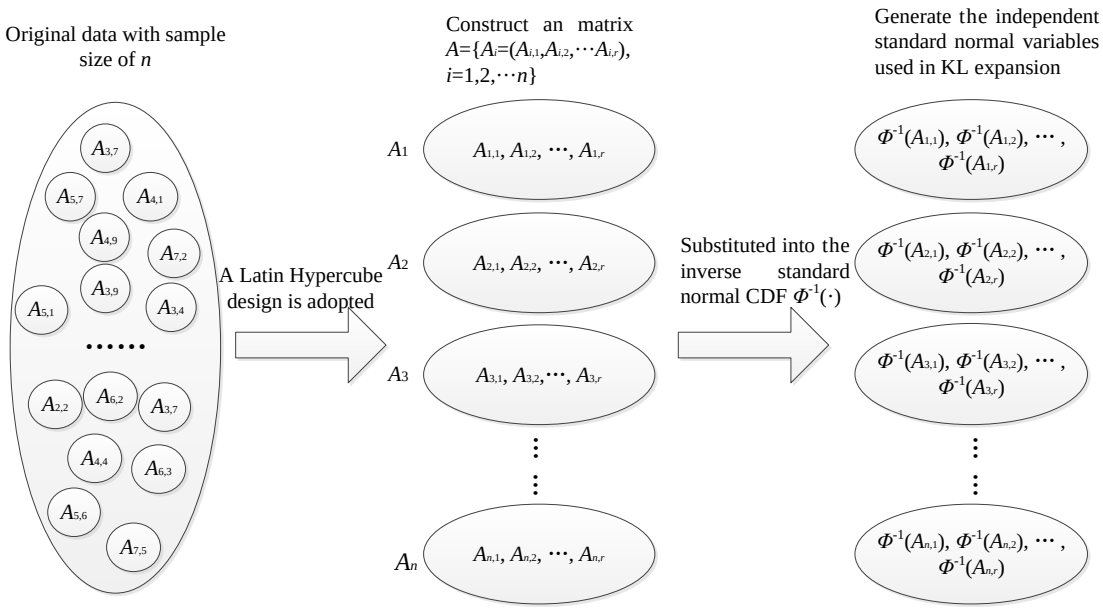

Figure 2. Concepts of quasi Monte-Carlo method.

Analysis of mean, variance, skewness, and kurtosis of response processes are shown as follows [20]:

$$\mu_X = \frac{1}{n \cdot N} \sum_{j=1}^{N} \sum_{i=1}^{n} X_i(t_j) \tag{11-1}$$

$$\sigma_X{}^2 = \frac{1}{n \cdot N} \sum_{j=1}^{N} \sum_{i=1}^{n} [X_i(t_j) - \mu_X]^2 \tag{11-2}$$

$$S_X = \frac{1}{n \cdot N} \sum_{j=1}^{N} \sum_{i=1}^{n} \left[(X_i(t_j) - \mu_X)/\sigma_X\right]^3 \tag{11-3}$$

$$K_X = \frac{1}{n \cdot N} \sum_{j=1}^{N} \sum_{i=1}^{n} \left[(X_i(t_j) - \mu_X)/\sigma_X\right]^4 \tag{11-4}$$

where $X_i(t_j)$ is the value of output process $X_i(t)$ at time instant t_j. Because outputs are stationary, their autocorrelation at a relative time τ_1 is determined by:

$$\rho_{XX}(\tau_1) = \frac{1}{n \cdot N_1} \sum_{j=1}^{N_1 \le N} \sum_{i=1}^{n} X_i(t_j) X_i(t_j + \tau_1) \tag{12}$$

where $N_1 = arg\ \underset{j}{max}\ [j | t_j + \tau_1 = (j-1) \cdot \Delta t + \tau_1 \le T, j = 1, \cdots N]$.

This paper uses numerical calculations to analyse outputs of a vehicle system under non-Gaussian inputs. The first four moments and autocorrelation of responses are estimated by Eq.(11) and (12), then output processes can be simulated based on PCE-KL expansion.

Analysis of PDF of Fatigue Life

When fluctuating stress is imposed on a vehicle component for a long time, there could appear fatigue damage or even failure. The relationship between the stress level S and the number of cycles N for the specimen to fail at the same stress level is expressed according to the S-N curve:

$$N \cdot S^a = b \tag{13}$$

where a and b, related to material properties, are constants. The Miner damage model is the simplest and most effective statistical way to describe cumulative damage. In the first place, the number of cycles n_k at a cyclic load S_k is estimated. When specimen appears fatigue failure under the stress level S_k, S-N curve is used to calculate the number of cycles N_k. Next, the incremental damage D_k is equal to n_k/N_k. Therefore, cumulative damage D can be presented by summing up D_k at various stress level:

$$D = \sum_k D_k = \sum_k \frac{n_k}{N_k} \tag{14}$$

where D is constant, and fatigue failure occurs if D is greater than 1 (D>1). In order to account for the mean stress effect, S in Eq.(13) is replaced by Se, which can be represented by the following Goodman model:

$$Se = S_a/(1 - S_m/S_u) \tag{15}$$

where S_a is the stress amplitude, S_m is the mean stress, and S_u is the ultimate strength of the material.

Rain-flow counting is a way to describe the statistical law of stress with time-varying. A series of stress trajectories $\tau_i(t)$, i=1,2,…,n are first simulated for the purpose of analysing fatigue life PDF. Each of them is rainflow counted, and Eq.(13), (14), (15) provide realizations of the incremental damage D_{ik}, k=1,2,…,m in ith stress trajectory. Then the PDF of fatigue life Y_i =1/D_i in seconds can be supplied by the saddlepoint approximation [21]. The followings are specific steps about SPA.

Saddlepoint approximations is an effective statistical method for obtaining probability density and distribution function approximation formulas. The PDF of stochastic variables Y=[Y_1, Y_2,⋯, Y_n] is $f_Y(y)$ and the moment generating function (MGF) of Y could be defined as:

$$\psi_Y(t) = E[e^{ty}] = \int_{-\infty}^{\infty} e^{ty} f_Y(y)dy = \frac{1}{n}\sum_{i=1}^{n} e^{t \cdot Y_i} \tag{16}$$

where t is in the neighbourhood of 0, as well as n is the number of sample points. The cumulant generating function (CGF) of Y is given by the natural logarithm of MGF, that is to say:

$$K_Y(t) = log[\psi_Y(t)] \tag{17}$$

Performing inverse Fourier transform on $\psi_Y(it)$, we can get the PDF of Y:

$$f_Y(y) = \frac{1}{2\pi}\int_{-\infty}^{\infty} e^{-ity}\psi_Y(it)dt = \frac{1}{2\pi}\int_{-i\infty}^{i\infty} e^{[K_Y(t)-ty]}\,dt \tag{18}$$

The integral in the above formula is estimated by the exponential power series expansion, then Eq.(18) is exchanged by:

$$f_Y(y) = \left[1/2\pi K_Y''(t_s)\right]^{1/2} e^{[K_Y(t_s)-t_s y]} \tag{19}$$

$K_Y''(\cdot)$ denotes the second derivative of CGF and t_s is the saddlepoint which is solved by the following equation:

$$K_Y'(t) = y \tag{20}$$

where $K_Y'(\cdot)$ is the first-order derivative of CGF of Y. Then the cumulant generating function of Y in Eq.(17) is replaced by the following formula:

$$K_Y(t) = \sum_{j=1}^{\infty} v_j \frac{t^j}{j!} \tag{21}$$

where v_j are jth cumulant of Y, the values of the first four cumulants are calculated as follows:

$$v_1 = \mu_Y \tag{22-1}$$
$$v_2 = \sigma_Y^2 \tag{22-2}$$
$$v_3 = S_Y\sigma_Y^3 \tag{22-3}$$
$$v_4 = (K_Y\text{-}3)\times\sigma_Y^4 \tag{22-4}$$

The mean μ_Y, variance σ_Y^2, skewness S_Y and kurtosis K_Y could be calculated. Based on this information, Eq.(20) is written as:

$$K_Y'(t) = v_1 + \sum_{j=2}^{4} v_j \frac{t^{j-1}}{(j-1)!} = y \tag{23}$$

SPA provides accurate probability estimation, especially in the left and right tail area of distribution. Besides, the analysis process is very simple, and the core of SPA is to find one saddle point without any integration.

SIMULATION AND RESULTS

In this paper, a quarter vehicle model (the tire damping is negligible) is simplified into a nonlinear vibration system under non-Gaussian loads, as shown in Figure 3.

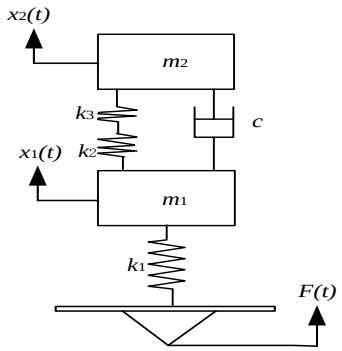

Figure 3. Model of the quarter vehicle suspension.

The differential equations of motion are recorded as:

$$\begin{aligned} m_1\ddot{x}_1 + c(\dot{x}_1 - \dot{x}_2) + (k_1 + k_2)x_1 - k_2x_2 + k_3(x_1 - x_2)^3 = k_1F \\ m_2\ddot{x}_2 - c(\dot{x}_1 - \dot{x}_2) - k_2(x_1 - x_2) - k_3(x_1 - x_2)^3 = 0 \end{aligned} \quad (24)$$

where $F(t)$ is a non-Gaussian road excitation. The masses m_1 and m_2 are respectively 80 and 350kg, the damping coefficient is c=12000kg/s, the spring rates are k_1=400kN/m, k_2=45kN/m. We consider a nonlinear hardening for the suspension spring, k_3=80kN/m. Shear stress working on the suspension is composed of two parts. One is static stress because of the weight of the vehicle, and another is alternating stress resulted from road excitation. The deflection of the spring (x_1–x_2) is calculated by the dynamic response of the vehicle system. Dynamic and static shear stress then are calculated as:

$$\tau = K_w \frac{8Dk_2(x_1 - x_2)}{\pi d^3} \quad (25)$$

$$\tau_m = K_w \frac{8Dm_2g}{\pi d^3} \text{ where } K_w = \frac{4C-1}{4C-4} + \frac{0.615}{C} \quad (26)$$

The coil and wire diameters D and d are 17.3 and 2.2cm, the spring index C is equal to 7.878, as well as gravitational acceleration is 9.8m/s^2 and the ultimate strength of the material S_u is 850MPa. In this model, total shear stress τ_u should be calculated by adding up static stress τ_m and dynamic stress τ. In Eq.(25) and (26), the Wahl factor K_w is used to account for the stress increase on the spring wire due to the spring curvature. Whether the road roughness is Gaussian or non-Gaussian process, its PSD [22] is:

$$S_F(w) = 4\pi^2 n_0{}^2 S_F(n_0) v/(w^2 + w_0{}^2) \quad (27)$$

where $S_F(n_0)$ is road roughness coefficient, n_0=0.1m^{-1} is standard spatial frequency, w is the circular road frequency, and w_0=2πvn_0, as well as v represents the vehicle speed which is equal to 60km/h. Table 1 presents different values of $S_F(n_0)$ according to the road classification from A to H, and type of road D is selected in this paper.

Table 1. Road classification rules.

Road classification	A	B	C	D	E	F	G	H
$S_F(n_0)/(\times 10^{-6}\,\mathrm{m}^3)$	16	64	256	1024	4096	16384	65536	262144

Figure 4 shows PSD of non-Gaussian excitation $F(t)$. Autocorrelation function $\rho_{FF}(\tau)$ was the inverse Fourier transform of $S_{FF}(w)$ and it's curve is shown in Figure 5. We toke vibratory time interval as [0, 50] sec which was discretized by Δt =0.01, so covariance matrix of the road profile C_{FF}=[$C_{FF}(t_i,t_j)$], i, j=1,⋯5001 was formed, apart from this, $C_{FF}(t_i,t_j)$ was equal to $\rho_{FF}(\tau)$ and τ=|t_i-t_j|=$\Delta t|i$-j|. The first four moments of non-Gaussian excitation were supposed as μ_F =0, $\sigma_F{}^2$=0.00032, S_F=1.3, K_F=7.6. Then calculating coefficients b_0,b_1,b_2,b_3 by Eq.(9) and (10), besides, $\boldsymbol{\Sigma}_{\xi\xi}$=[$\boldsymbol{\Sigma}_{\xi\xi}(t_i,t_j)$], i, j=1,2,⋯,5001 of the Gaussian process $\xi(t)$ in PCE was constructed based on the definition of covariance matrix C_{FF} and Eq.(7).

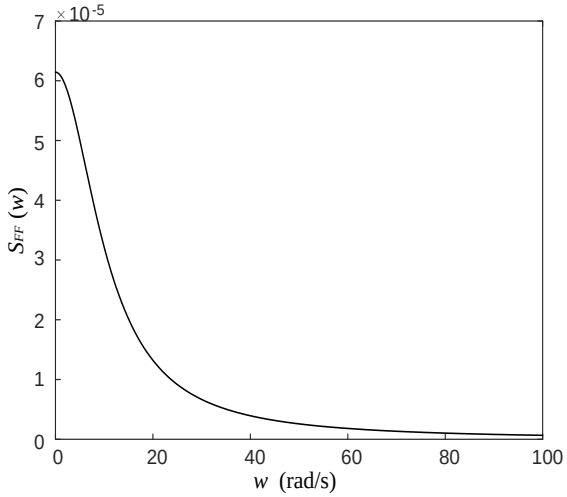

Figure 4. PSD of $F(t)$.

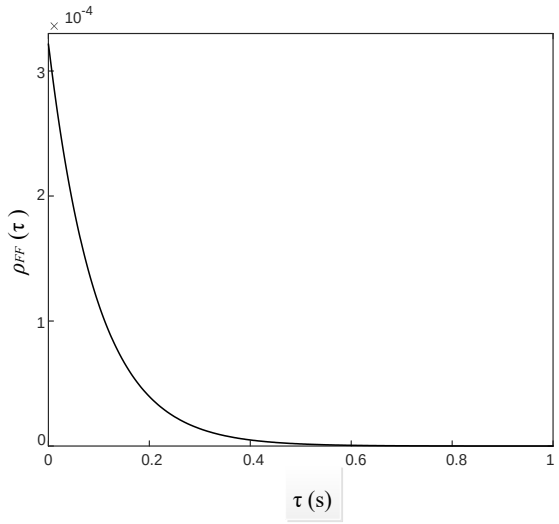

Figure 5. Autocorrelation values of $F(t)$.

Performing spectral decomposition to obtain eigenvalues based on Eq.(1) and these eigenvalues which were sorted from large to small were in turn recorded as $\boldsymbol{\lambda_i}$, i=1,2,⋯,5001. Figure 6 presents the partial eigenvalues of $\boldsymbol{\Sigma}_{\xi\xi}$. Then, the principal component analysis was executed, and p was 0.95. According to Eq. (3), r was 1903. In order to acquire random process $\xi(t)$, these values, i.e. singular values λ_i, vectors Q_i and standard normal random variables ξ_i, i=1,2,⋯,r generated by QMC, were substituted into Eq.(2). Subsequently, substituting $\xi(t)$ into Eq.(6) to generate a non-Gaussian process $F(t)$. Figure 7 shows the trajectory of a non-Gaussian road profile.

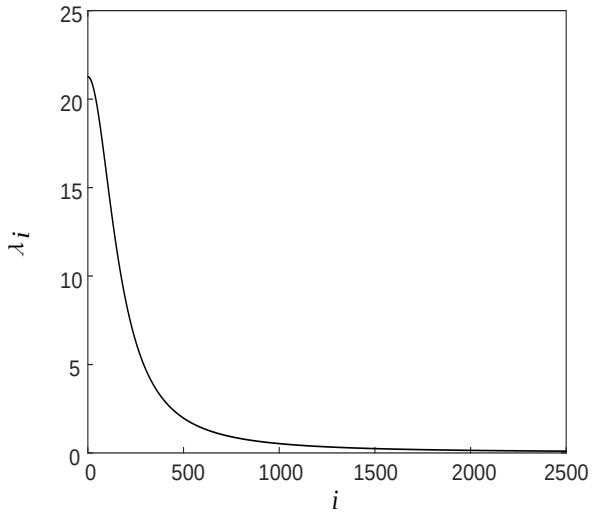

Figure 6. Eigenvalues of $\Sigma_{\xi\xi}$.

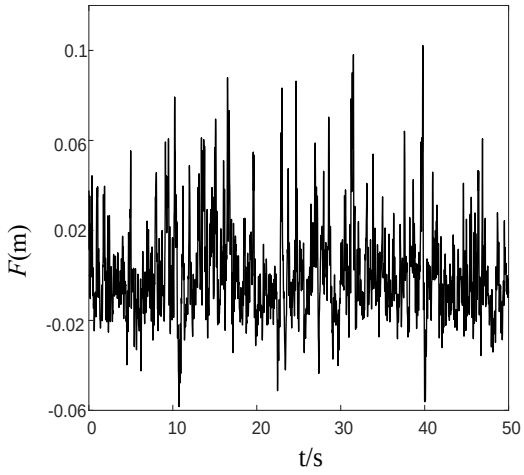

Figure 7. A trajectory of $F(t)$.

Table 2. Analysis of characteristic statistical parameters of the non-Gaussian process.

Sample points	Mean	Variance	Skewness	Kurtosis
10^3(QMC)	0	0.00032	1.2537	7.0280
5×10^3	0	0.00032	1.2754	7.2776
10^4	0	0.00032	1.2903	7.4147
10^6(MC)	0	0.00032	1.2985	7.5621
Real values	0	0.00032	1.3	7.6

In order to illustrate the effectiveness of the quasi Monte Carlo method, this paper simulated non-Gaussian inputs using a different number of sampling points. Then calculating values of the first four moments and comparing them with actual values, as well as the analysis results are shown in Table 2. It can be seen that the application of quasi-Monte Carlo greatly reduces the number of samples. Based on the fourth-order Runge-Kutta method and $F(t)$, Eq. (24) was integrated numerically to obtain outputs $X_1(t)$ and $X_2(t)$. Table 3 gives values of the first four moments about outputs, and the autocorrelation curve of response processes $X_1(t)$ and $X_2(t)$ is presented in Figure 8. Figure 9 shows a pair of representative responses $X_1(t)$ and $X_2(t)$, which create a dynamic shear stress τ because of differences between them.

Table 3. The first four moments of output processes X_1(t) and X_2(t)

The moments of outputs	Mean	Variance	Skewness	Kurtosis
X_1(t)	0	0.00042	1.1540	6.5276
X_2(t)	0	0.00039	1.1237	6.2931

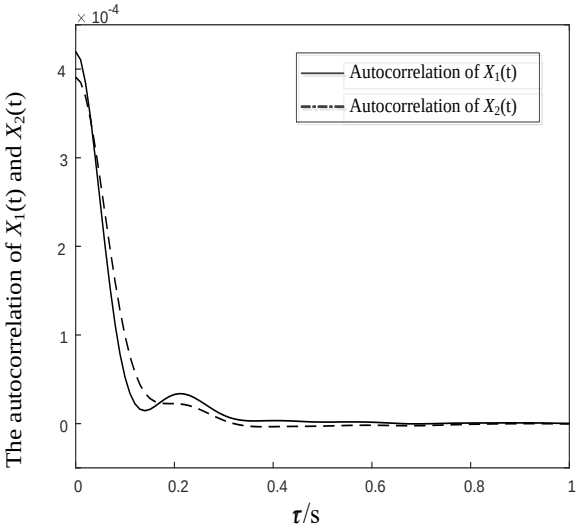

Figure 8. Autocorrelation functions of outputs.

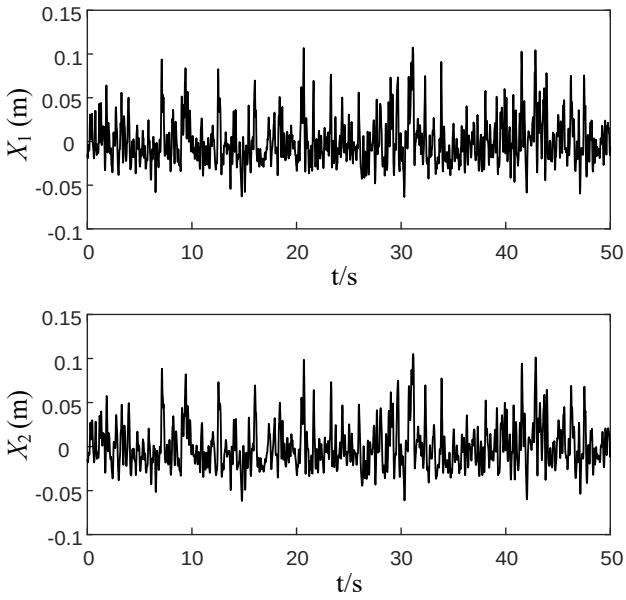

Figure 9. Output processes.

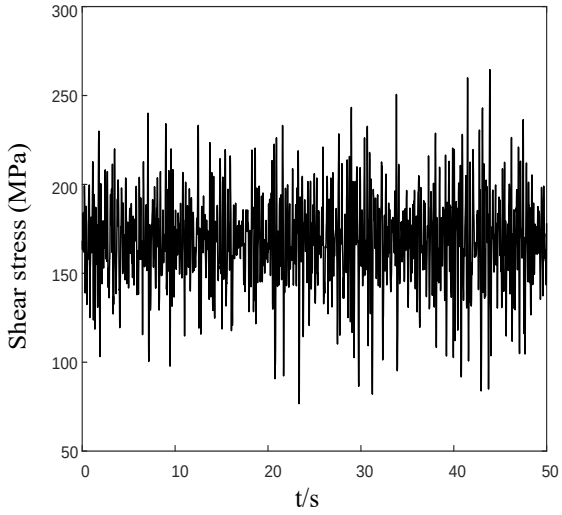

Figure 10. A representative trajectory of shear stress.

According to Eq. (25) and Eq. (26), the total stress was represented as $\tau_u(t)=\tau_m+\tau(t)$ where static component τ_m was 168 MPa. A representative trajectory of total shear stress is presented in Figure 10. The non-Gaussian dynamic shear stress simulation process was repeated for 10^4 times, and the first four moments of total shear stress $\tau_u(t)$ are shown as Table 4 based on these stress trajectories. Figure 11 is the PDF of non-Gaussian shear stresses.

Table 4. First four moments of shear stress process.

The first four moments	Mean	Variance	Skewness	Kurtosis
values	168	456	-0.4315	5.3720

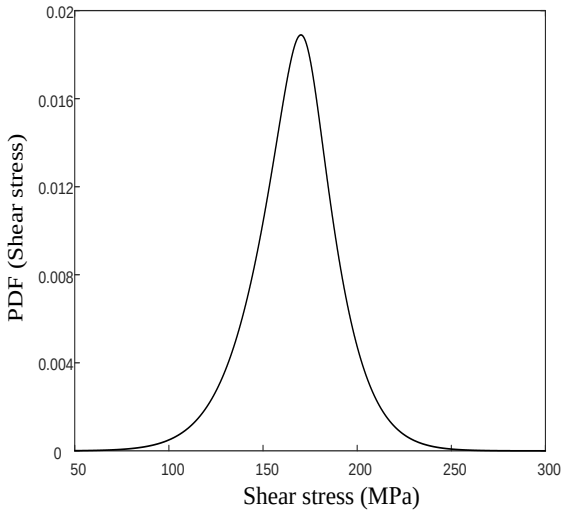

Figure 11. PDF of non-Gaussian shear stresses.

Every simulated non-Gaussian shear stress trajectory was rainflow cycle counted to calculate the corresponding cumulative damage per second on the basis of Eq. (13) to Eq. (15).

Table 5. Stochastic parameters in the *S*-*N* curve.

Variable	Mean	Variance	Distribution
a	6.1	2.5% mean	Normal
b	1.02×10^{17}	2.5% mean	Normal

The fatigue strength exponent *a* and fatigue coefficient *b* in *S*-*N* curve were considered as Gaussian variables to account for the inherent variability in material properties and test conditions. These random parameters are presented in Table 5. Finally, the SPA method was used to estimate the PDF using 10^4 fatigue life samples. The replacement frequency of automobile suspension spring in this article is generally between three and five years, which is basically consistent with the main concentrated area of fatigue life in Figure 12.

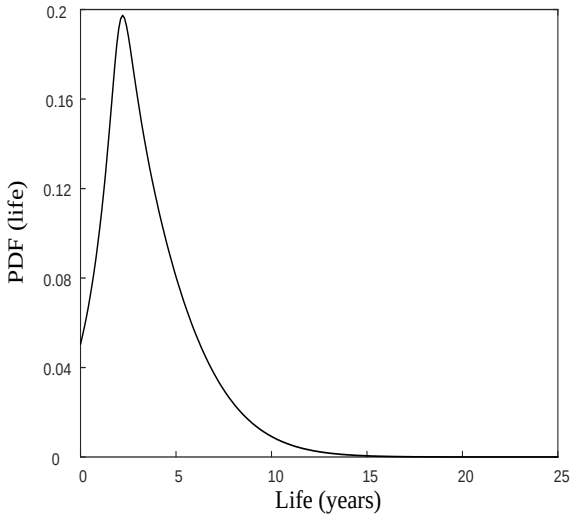

Figure 12. PDF of fatigue life.

CONCLUSION

Fatigue life estimation plays an important role in the manufacturing and operating of a vibratory system. In a real environment, a system usually experiences non-Gaussian excitation, which is obviously different from Gaussian type. So these fatigue life estimation approaches based on the Gaussian stress assumption theory cannot provide accurate fatigue life. This paper presented a numerical methodology to simulate non-Gaussian excitation accurately as well as calculate the fatigue life of a vehicle system efficiently.

A non-Gaussian incentive was simulated by polynomial chaos expansion, Karhunen-Loeve expansion and quasi Monte Carlo approach on the foundation of the given first four moments and PSD. Because the original Monte Carlo analysis has heavy tasks of calculations, quasi Monte Carlo, which can reduce the workload of numerical simulation is adopted to improve computational efficiency in this paper. In high-dimensional random variables space, the simulation results quickly converge to the true value by reasonably sampling and controlling the distribution of random variables.

The non-Gaussian processes, statistical information and autocorrelation structure of responses should be analysed by simulating stochastic inputs. Then, every output stress was rainflow cycle counted to calculate the corresponding cumulative damage random variables based on the Miner damage model and *S*-*N* curve. Ultimately, the SPA provided PDF of fatigue life, which gave not only the expected life but also some important statistics, such as low and high percentiles.

The proposed way accurately predicts the fatigue life of vibratory systems under non-Gaussian loads, as well as an example was given to verify the feasibility of the above theory according to the suspension of a quarter vehicle under non-Gaussian loads.

REFERENCES

[1] Tallia R, Morello P, Castellano G. Damage and failure of composite materials. AIAA Journal 2012; 52(5): 317-323.

[2] Husaini, Putra TE, Ali N. Fatigue feature clustering of modified automotive strain signals for saving testing time. International Journal of Automotive and Mechanical Engineering 2018; 15(2): 5251-5272.

[3] Zhu DP. Digital generation of non-Gaussian random vibration signals in railway transportation and package response analysis. Concurrency Computat Pract Exper 2018; 31(10): 1-9.

[4] Tsianika V, Geroulas V, Mourelatos ZP, et al. A methodology for fatigue life estimation of linear vibratory systems under non-Gaussian loads. SAE International Journal of Commercial Vehicles 2017; 10(2): 460-472.

[5] Bocchini P, Deodatis G. Critical review and latest developments of a class of simulation algorithms for strongly non-Gaussian random fields. Probabilistic Engineering Mechanics 2008; 23(4): 393-407.

[6] Liu ZJ, Liu ZX, Peng YB. Dimension reduction of Karhunen-Loeve expansion for simulation of stochastic processes. Journal of Sound and Vibration 2017: 408:168-189.

[7] Papaioannou G, Dineff A, Koulocheris D. Comparative study of different vehicle models with respect to their dynamic behavior. International Journal of Automotive and Mechanical Engineering 2019; 16(3): 7061-7092.

[8] Quigley JP, Yung LL, Liang W. Review and assessment of frequency-based fatigue damage models. SAE International Journal of Materials & Manufacturing 2016: 9(3): 565-577.

[9] Vantadori S, Iturrioz I, Ronchei C. Discussion on fatigue life estimation under multiaxial random loading: Comparison between time-and frequency-domain approach. Theoretical & Applied Fracture Mechanics 2018; 96: 134-145.

[10] Thorsen MJ, Saevik S, Larsen CM. Fatigue damage from time domain simulation of combined in-line and cross-flow vortex-induced vibrations. Marine Structures 2015; 41: 200-222.

[11] Dietz S, Netter H, Sachau D. Fatigue life predictions of a railway bogie under dynamic loads through simulation. Vehicle System Dynamics 1998; 29(6): 385-402.

[12] Men YZ, Yu HB, Pan X, et al. Study on fatigue life of spring bracket for air suspension system. Advanced Materials Research 2012; 590: 372-376.

[13] Ferreira W, Meehan T, Cardoso V, et al. A comparative study of automotive system fatigue models processed in the time and frequency domain. SAE Technical Paper: 010377; 2016.

[14] Kihm F, Halfpenny A, Munson K. Synthesis of accelerated and more realistic vibration endurance tests using kurtosis. SAE Technical Paper: 010275; 2016.

[15] Mourelatos ZP, Majcher M, Pandey V, et al. Time-dependent reliability analysis using the total probability theorem. Journal of Mechanical Design 2015; 137(3): 031405.

[16] Xiu D, Karniadakis G. The Wiener-Askey polynomial chaos for stochastic differential equations. SIAM Journal on Scientific Computing 2002; 24(2): 619-644.

[17] Peter JM, Laarhoven V, Emile HL. Simulated annealing: theory and applications. 1st ed. Berlin: Springer Netherlands; 1987.

[18] Husnain MNM, Akramin MRM, Chuan ZL, et al. Fatigue crack growth analysis using Bootstrap S-version finite element model. Journal of the Brazilian Society of Mechanical Sciences and Engineering 2020; 42(4).

[19] Zhang H, Dai H, Beer M, et al. Structural reliability analysis on the basis of small samples: an interval quasi-Monte Carlo method. Mechanical Systems and Signal Processing 2013; 37(1-2):137-151.

[20] Geroulas V, Mourelatos ZP, Tsianika V. Reliability analysis of nonlinear vibratory systems under non-Gaussian loads. Journal of Mechanical Design 2018; 140(2): 021404.

[21] Huang B, Du X, Lakshminarayana RE. A saddlepoint approximation based simulation method for uncertainty analysis. International Journal of Reliability and Safety 2006; 1(1/2):206.

[22] ISO 8608. Mechanical vibration. Road surface profiles. Reporting of measured data, 1st ed. 1995.